BJPS

Brazilian Journal of Pharmaceutical Sciences

http://dx.doi.org/10.1590/s2175-97902019000418579

Article

Targeting of temozolomide using magnetic nanobeads: an *in vitro* study

Berna Gürten[1], Elçin Yenigül[1], Ali Demir Sezer[2*], Cem Altan[1], Seyda Malta[1]

[1]Department of Chemical Engineering, Faculty of Engineering, Yeditepe University, Ataşehir, Istanbul, Turkey, [2]Department of Pharmaceutical Biotechnology, Faculty of Pharmacy, Marmara University, Haydarpaşa, Istanbul, Turkey

Temozolomide, a chemotherapeutic drug that is often administered for the treatment of brain cancer has severe side effects and a poor aqueous solubility. In order to decrease the detrimental effect of the drug over healthy cells, a novel drug delivery vehicle was developed where the therapeutic drug was encapsulated within the hydrophobic cavities of β-CD modified magnetite nanoparticles, which are embedded in chitosan nanobeads prepared by salt addition. *In-vitro* studies have shown that the magnetic properties of the novel delivery vehicle are adequate for targeted drug delivery applications under an external magnetic field. Additionally, an increase in the amount of chitosan was shown to exhibit a strong shielding effect over the magnetic properties of the delivery vehicle, which lead to deterioration of the amount of captured drug at the targeted area, suggesting a delicate balance between the amounts of constituents composing the drug delivery vehicle.

Keywords: Temozolomide. Magnetite. Cyclodextrin. Chitosan. Targeting. Anticancer.

INTRODUCTION

Chemotherapy is still the most widely used therapeutic approach in the management of cancer, in combination with surgery and radiation therapy. Temozolomide (TMZ), is a second generation imidazotetrazinone derivative with methylating properties, used as an oral cytotoxic agent for the adjuvant chemotherapy of malignant primary brain tumors, namely glioblastoma (Stupp *et al*., 2005) and malignant glioma (glioblastoma multiforme and anaplastic astrocytoma) (Brada *et al*., 1999; Marchesi *et al*., 2007). The drug contains an imidazole group, which connects to a tetrazine ring. TMZ is presumed to have antitumor ability in the metabolism via chemical decomposition of the substance to 3-methyl-(triazen-1-yl) imidazole-4-car-boxamide (MTIC), which is assumed to alkylate nucleophiles (Kim *et al*., 2001). This process is highly pH dependent since TMZ exerts its in-vivo activity by spontaneous hydrolyzation at physiologic pH (Andrasi *et al*., 2010). Further studies in rats and rhesus monkeys have shown that the level of TMZ in the cerebrospinal and brain are 30-40% of plasma concentration (Agarwala, Kirkwood, 2000). Temozolomide brings extensive additional benefits of crossing the blood brain barrier to its analogues DTIC (5-(3, 3-dimethyl-1-triazenyl) imidazole-4-carboxamide), another member of the class of alkylating agent, which has a similar mechanism of action to metastatic melanoma that frequently metastasizes to the brain (Zuckerman *et al*., 2011). Additionally, Baker *et al*. (1999), conducted a study with 14C-TMZ in cancer patients and observed that a low interpatient variability in TMZ clearance suggests that TMZ administration will result in efficient generation of the active metabolite MTIC in all tissues where TMZ is present, which supports further therapeutic advantage of TMZ (Baker *et al*., 1999).

Aqueous solubility is considered as one of the major concerns of conventional chemotherapy as a result of

***Correspondence:** A.D. Sezer, Department of Pharmaceutical Biotechnology, Marmara University, Haydarpaşa 34668, Istanbul, Turkey. Tel: +90 216 414 29 63, Fax: +90 216 345 29 52. E-mail: adsezer@marmara.edu.tr

the mostly nonpolar characteristics of chemotherapeutic agents (Chidambaram, Manavalan, Kathiresan, 2011). Therefore, suitable delivery vehicles should be used to increase the solubility and the selectivity of conventional chemotherapeutic agents. Along with solubility, chemical stability of TMZ is also important. Once TMZ is delivered in the body, it quickly decomposes to its active agent, MTIC due to the neutral pH. Therefore, any delivery vehicle of the drug should be prepared in acidic solution and then lyophilized for stability. In some drug delivery systems, cyclodextrins (CDs) have been used to form inclusion complexes in order to increase the solubility of poorly soluble drugs, and enhance their bioavailability and stability (Tiwari, Tiwari, Rai, 2010). CDs are cyclic oligosaccharides which contain at least six D-(+) glucopyranose units attached by α-(1, 4) glycosidic bond (Eastburn, Tao, 1994). Due to their strong intermolecular hydrogen bonding, they have restricted solubility in aqueous medium. Replacement of the H-bond of the structure forming –OH group helps to enhance their solubility (Hakkarainen *et al*., 2005). Therefore, various derivatives of CDs are investigated such as hydroxyl-propyl derivatives and methylated β-CDs, etc (Del Valle, 2004). TMZ is shown to form inclusion complexes with different types of CDs and an increase in solubility during complex formation has been reported (Huang *et al*., 2008; Jain, Gursalkar, Bajaj, 2013; Swaminathan, Cavalli, Trotta, 2016).

Many serious side effects of chemotherapeutic drugs are widely presented in the literature (Hamzelou, 2017; Coolbrandt *et al*., 2011; Bagot, 2015; Song *et al*., 2014). Drug delivery systems have been developed in order to reduce these side effects and minimize the amount of drug administered to the human body. As these systems minimize the non-specific distribution of the drugs within the body causing invasion of healthy cells together with tumor cells, they enhance the efficiency of therapy and decrease the dose of the drug. The drug delivery systems are mainly composed of nanocarriers with core/shell structures. Amongst the many reported nanocarriers, magnetic nanoparticles predominantly iron oxides, are widely used due to their biocompatibility (Janko *et al*., 2017; Shaterabadi, Nabiyouni, Solymani, 2017; Patil *et al*., 2014). Moreover, it is possible to manipulate organization of the magnetic nanoparticles in solution by applying an external magnetic field, which allows for the needed accumulation of the particles as well as chemotherapeutic drugs at the tumor site. Magnetite (Fe_3O_4), which is also known as black iron oxide, is a naturally occurring mineral and exhibits the strongest magnetism of any transition metal oxide (Scwertmann, Cornell, 2006; Andrade-Eiroa *et al*., 2016). Additionally, magnetite is non-toxic, highly biocompatible and biodegradable, all of which make it a favorable candidate as a nanocarrier for targeted drug delivery systems (Kumar, Inbaraj, Chen, 2010). However, the overall performance of the drug delivery system containing magnetic nanoparticles as a transporter relies on the size, morphology and the magnetic properties of magnetite nanoparticles, as these properties affect the overall external targeting performance. Moreover, applied field strength as well as depth of the target tissue, rate of blood flow, and vascular supply play a role in the effectiveness of the corresponding drug delivery system. Most importantly, magnetite nanoparticles can also be used in parallel therapeutic approaches for cancer where particles can be targeted to the tumor site for hyperthermia, while active compound can be loaded onto the surface of the particles for drug delivery and specific antibodies can be conjugated for targeting purposes (Sun, Lee, Zhang, 2008).

In the core-shell structure of a drug delivery vehicle, apart from the core, a suitable shell also plays an important role. Chitosan is an amphiphilic, natural, non-toxic and biocompatible polymer which is reported to enhance the solubility of poorly soluble hydrophobic chemotherapeutic drugs such as paclitaxel, camptothecin and doxorubicine in drug delivery systems (Nam *et al*., 2013; Bano *et al*., 2016; Qi *et al*., 2010). In addition to this effect over the solubility of the chemotherapeutic drugs, the polymeric chitosan micelles help passive targeting at the tumor site due to improved retention (EPR) effect and permeability (Riva *et al*., 2011), all of which make chitosan a suitable polymeric shell around the magnetic core for targeted drug delivery systems.

In this study, a new drug delivery system is developed for a chemotherapeutic agent, TMZ, using magnetic nanoparticles, CDs and chitosan to obtain a core-shell structure that can be manipulated by applying an external magnetic field. For this purpose, magnetite nanoparticles, which are coated with CDs, are synthesized by chemical co-precipitation method. Magnetite-chitosan nanobeads are synthesized by the ionic gelation method using these CD-coated magnetite nanoparticles. Finally, TMZ is incorporated in the chitosan-magnetite nanobeads to obtain the magnetic drug delivery system.

MATERIAL AND METHODS

Material

FeCl3 (anhydrous, 97%), FeSO4.7H2O (90%) and NaOH (99%) used in the synthesis of magnetite were obtained from Riedel-de Haen. TMZ (99.38%) was obtained from Koçak Farma (İstanbul, Turkey) as a gift and was used as received. Hydrochloric acid (37%, Sigma Aldrich), acetic acid (≥99.8%, Sigma Aldrich), methanol (99.7%, Sigma Aldrich) were used as received. β-Cyclodextrin (β-CD), Hydroxypropyl-β-Cyclodextrin (H-β-CD), Hydroxypropyl-γ-Cyclodextrin (H-γ-CD) were purchased from Sigma Aldrich. In addition, medium molecular weight chitosan (Sigma Aldrich), Sodium Sulfate Decahydrate (99%, Sigma Aldrich) (Na2SO4.10H2O) were used. The water used was distilled by reverse osmosis using GFL 2004.

The cell line used in this study, Human umbilical vein endothelial cells (HUVEC), was obtained from the American type Culture Collection Corporation (ATCC-CRL-1730, Virginia, USA). The Dulbecco Eagle's Minimum Essential Medium (DMEM; contains L-Glutamine, Gibco) was used. Infection of the cells was prevented using antimycotic (Anti-Anti (100X), Gibco) that was added to the medium as an antibiotic. Fetal bovine serum (FBS) was supplied from Gibco. Dulbecco's Phosphate Buffered Salt Solution (DPBS; w/o: Calcium, w/o: Magnesium) was from PAN Biotech, GmbH. Dimethyl sulfoxide (DMSO) was supplied from Sigma-Aldrich, UK. Additionally, tetrazolium salt (MTS) was purchased from Promega Corporation (CellTiter 96®Aqueous MTS Reagent Powder). HUVEC's were grown in DMEM (1X) with high glucose content (4.5 g/L) medium that contains %10 FBS, %1 penicillin-streptomycin and %1 antimycotic. The cells were used in the logarithmic phase of growth and maintained at 37 ºC in humidified 5% CO2 and 95% air.

METHODS

Synthesis of magnetite nanoparticles with β-CD, H-β-CD and H-γ-CD

The synthesis of bare magnetite nanoparticles was carried out by the chemical co-precipitation method with some modifications (Petcharoen, Sirivat, 2012). In a typical synthesis, 0.242 g FeSO4.7H2O and 0.282 g FeCl3 were dissolved in 80 mL de-aerated water along with 0.5 g β-CD. After complete mixing under mechanical stirring, while heating to 80 ºC and streaming N2(g) through the solution, 20 mL of 2.57 wt. % NaOH solution was quickly added to obtain a black suspension and the suspension was kept at 80 ºC for another 30 minutes under N2(g). After cooling to room temperature, magnetic nanoparticles were collected with magnetic separation and the nanoparticles obtained were washed with water. The concentration of the obtained magnetite solution was determined by Tiron chelation test (Yoe, Jones, 1944). The obtained nanoparticles were characterized as described elsewhere (Kleine *et al*., 2014). The same synthesis procedure was applied for the synthesis of magnetic nanoparticles which were functionalized with H-β-CD and H-γ-CD.

Characterization of magnetic nanobeads

The amounts of CDs on the surface of magnetite nanoparticles after synthesis are determined by using thermogravimetric analysis (TGA). TGA of the magnetite particles with and without cyclodextrins and only TMZ, only β-CD, TMZ-b-CD complex and TMZ-b-CD physical mixture are performed using a Perkin Elmer thermogravimetric analyzer at a heating speed of 10/min under nitrogen, where the temperature changes from 25 to 600 ºC . All samples are dried in a vacuum oven or by a freeze-dryer (SCANVAC, coolsafe) overnight. The size and morphology of the obtained magnetic nanobeads were investigated using a Scanning Electron Microscope (SEM) after being freeze-dried. Before measurement, the beads are coated with a thin layer of gold. The SEM used was a JEOL Ltd., JSM-5910LV at Boğaziçi University Advanced Technologies Research Center. The size distribution of these nanobeads was determined by Dynamic Light Scattering (DLS) taking an average of 10 consecutive measurements. The magnetic properties of the dried magnetic nanobeads are determined by Vibrating Sample Magnetometer (VSM). The instrument used was LDJ electronics 9600 and the measurements were taken between -15000 and +15000 Oe.

Formation of magnetite-chitosan nanobeads with TMZ

The size and size distribution of the obtained particles are optimized by varying the nature of the salts (TPP and Na2SO4 were employed), its concentration, how the magnetite nanoparticles are introduced and the concentration of chitosan. While some of these procedures lead to the formation of undesired products, an optimized procedure can be described as follows. Chitosan in 1% acetic acid solution was prepared and a pre-determined amount of solid TMZ (0.01 g) was added, vortexed and sonicated for one minute followed by magnetic stirring for 30 minutes (chitosan-TMZ solution). 2.1 mg/mL aqueous magnetite solution was added to the aqueous Na2SO4.10H2O solution to obtain the final desired salt concentration (1.1 or 2.2 wt.% salt). While being magnetically stirred, the chitosan-TMZ solution was added dropwise by a Hamilton syringe to the magnetite-salt solution over one minute and the final solution is stirred for another 30 minutes. The obtained solution was then centrifuged at 6000 rpm for 15 minutes and the precipitated chitosan-magnetite nanobeads were collected. The amount of TMZ in the nanobeads was calculated by measuring the remaining TMZ amount in the supernatant using HPLC.

Targeting of TMZ with magnetic nanobeads

In order to explore the possibility of targeting magnetite-chitosan beads containing the chemotherapeutic agent TMZ, an *in vitro* experimental setup consisting of a peristaltic pump providing a constant flow of 55 mL/min within 1.5 – 2 mm diameter tubing of 1 m length was prepared as shown in Figure 1. Additionally, handheld magnets generating a 0.3 – 0.5 T magnetic field were fixed at the test section, in order to collect magnetite-chitosan beads containing chemotherapeutic agent TMZ during the flow.

The magnetic nanofluid was circulated continuously through the system for one hour in the presence of an external magnetic field applied at the test section. The magnets were then removed and the captured magnetite nanoparticles were collected by passing 1 M HCl solution from the system. The amount of magnetite nanoparticles captured in the test section was calculated by carrying out Tiron chelation test (Yoe, Jones, 1944) and the amount of TMZ captured at the targeted area was determined using HPLC.

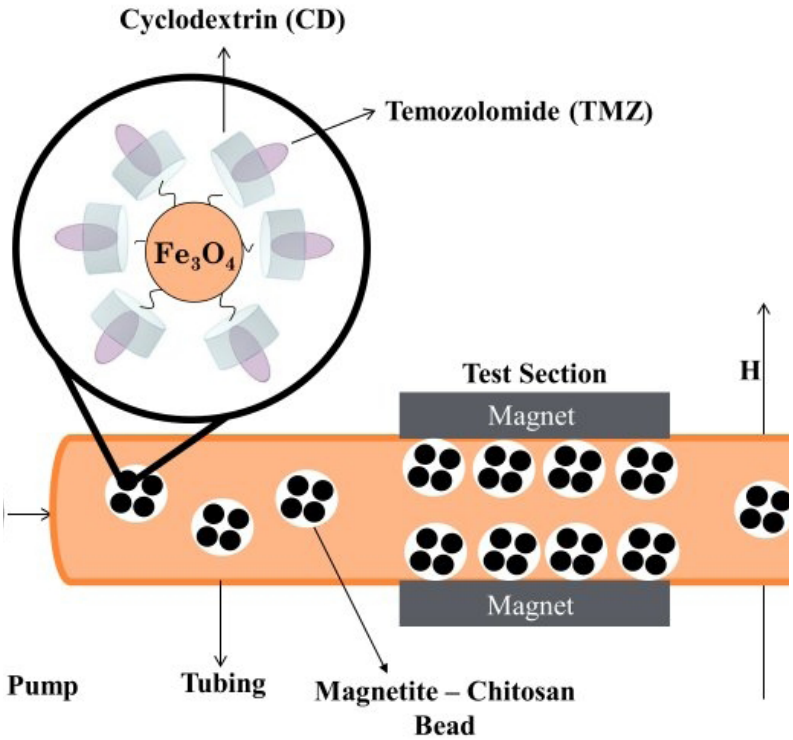

FIGURE 1 - Schematic diagram of the targeting study. TMZ incorporated magnetic nanobeads are circulated via peristaltic pump and collected at the target site by using an external magnetic field.

Quantification of TMZ by HPLC method

The HPLC method to quantify TMZ, which is given in detail elsewhere, was used with some modifications (Kim *et al*., 2001). Briefly, the HPLC system consists of 1525 Binary Pump, 2487 UV-Vis Detector, 717 Autosampler and a thermal column manager unit. X-Bridge 150 x 4.6, .5µm column was used and software was used to process the raw data. In HPLC, reverse phase C18 column (X-Bridge 150mmx .6cm, .5µm, Waters) was used. Water that contained 0.5 vol.% acetic acid/methanol (80:20 v/v) was prepared for the mobile phase. A standard calibration curve was obtained with five different TMZ concentrations (R2=0.998) and three injections of three different samples were measured. Prior to measurement, the magnetite in the system was removed upon addition of 1 M HCl to convert all the iron content of Fe_3O_4(s) to Fe+3 (aq), which takes place overnight, as the presence of nanoparticles interferes with the HPLC measurements and clogs the column. 1 M HCl also helps to maintain the chemical stability of TMZ until the HPLC measurements.

Cell viability assay

To evaluate *in vitro* cytotoxicity of chitosan coated magnetite nanoparticles, the tetrazolium salt based assay [3-(4,5-dimethylthiazol-2-yl)-5-(3-carboxymethoxyphenyl)-2-(4-ulfophenyl)-2H-tetrazolium, inner salt (MTS)] was employed. MTS is the name given to a colorimetric technique for assessing cell viability. Viable cells take up the MTS into their mitochondria in the presence of phenazine methosulfate (PMS) and metabolize it into blue formazan crystals, which can be spectrophotometrically quantified. MTS was performed to interpret the cell viability where 5x103 cells were inoculated in 100 µL of media, into each well of a 96-well plate, and left to incubate overnight to achieve sufficient cell attachment to the plate surface. Magnetite-chitosan nanobeads were dissolved in cell media for various nanoparticle solution concentrations (0.2%, 0.1%, 0.05%, 0.025% and 0.0125% (w/w)) and filtered through 0.2 µm filter, before being introduced to the plates. The media on the cells were then aspirated. 100 µL of suspension containing magnetite-chitosan nanobeads were added and incubated for additional 24 h, 48 h and 72 h in different well-plates. At each time interval, the supernatant was carefully removed and 110 µL of MTS solutions were added to the plates for an additional two-hour incubation. The MTS assay was performed in 4 replicates. Additionally, background correction was performed due to the dark color of magnetite nanoparticles in the medium. For background correction, four additional wells were employed as controls, which contained the same amounts of cells and the particles underwent the same treatment steps, but did not received the MTS solution. The absorption values obtained from these wells were subtracted from those of the sample wells.

RESULTS AND DISCUSSION

Size and morphology of chitosan-magnetite nanobeads

The morphology and the size of chitosan nanobeads containing functionalized magnetite nanoparticles were investigated by Scanning Electron Microscope (SEM). Figure 2 shows SEM images of chitosan nanobeads prepared by TPP and Na2SO4.10H2O salts, latter also in the absence and presence of magnetic nanoparticles which were incorporated into the nanobeads. SEM results clearly indicate that chitosan nanobeads could not be formed in the presence of TPP salt while the use of Na2SO4.10H2O lead to the formation of roughly 300 nm nanobeads which have irregular morphologies and wide size distribution. It appears that the particles adhere to each other upon drying as no individual particles can be identified with SEM. However, the DLS results as will be discussed shortly prove that in solution nanobead formation has taken place. SEM images also revealed that the incorporation of magnetite nanoparticles into the nanobeads remarkably decreased the average size of the nanobeads (20 nm, Figure 2c). As a consequence, utilization of Na2SO4 salt as the precipitating agent lead to the formation of magnetic nanobeads with satisfactory sizes and morphologies as stated in the literature (Parida, Bindhani, 2015; Saita *et al*., 2011).

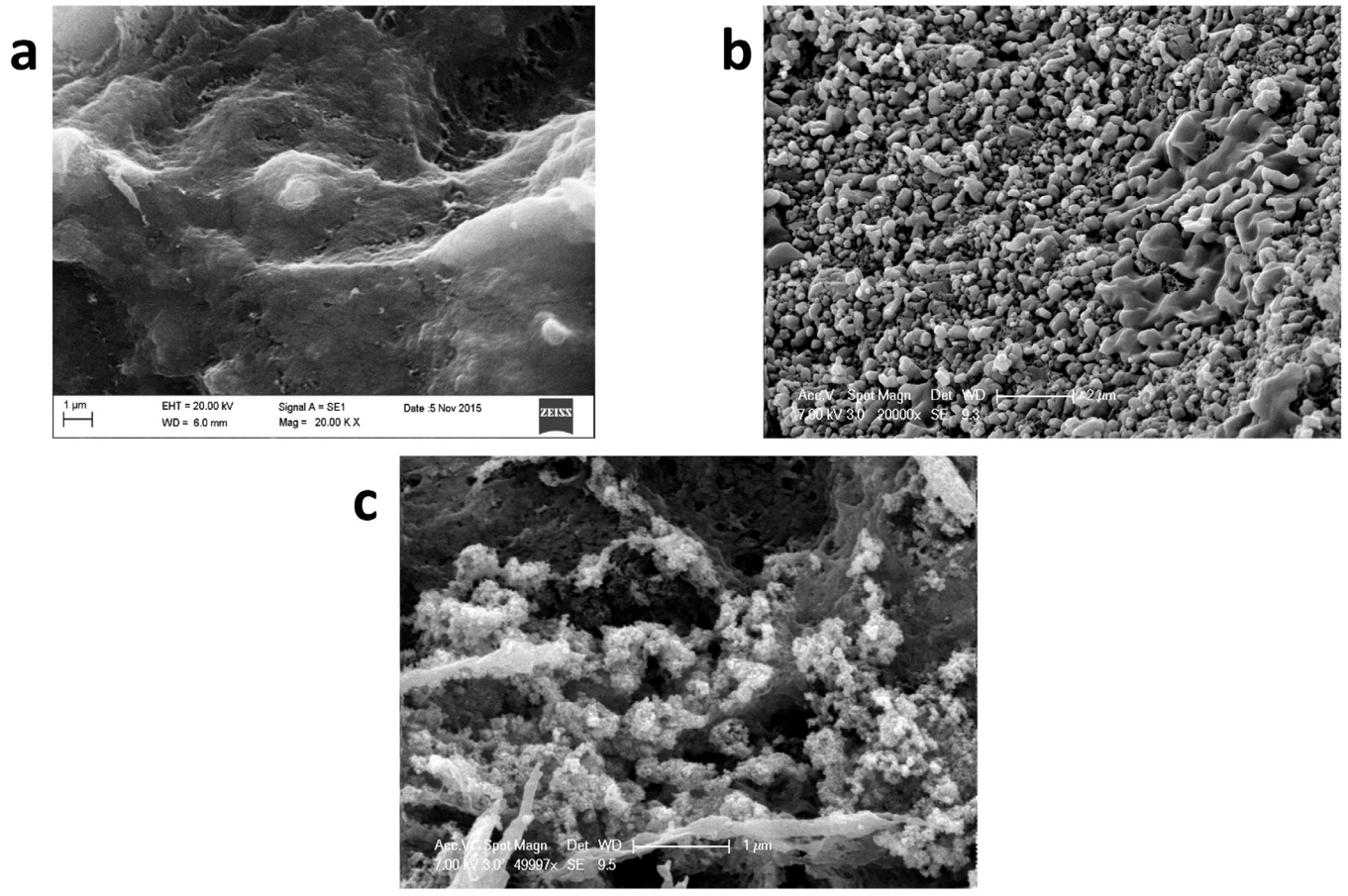

FIGURE 2 - SEM images of chitosan nanobeads (a) Chitosan nanobeads could not be formed in the presence of TPP salt (b) Roughly 300 nm of chitosan nanobeads were formed in the presence of $Na_2SO_4.10H_2O$ salt which have irregular morphologies and wide size distribution (c) Chitosan nanobeads formed in the presence of $Na_2SO_4.10H_2O$ salt, and magnetite nanoparticles have comparably smaller size (20 nm).

Size distribution of chitosan- magnetite nanobeads

Size distributions of magnetite-chitosan nanobeads with varying chitosan concentrations were investigated by DLS. According to the results given in Figure 3, the majority of the magnetite-chitosan nanobeads with the final concentration of 0.11 wt% have an average hydrodynamic diameter of 31±2 nm. Additionally, a minor aggregation is suggested by the intensity average plot, as another peak around 45 nm is obtained. These values are consistent with SEM images, where reduction of size is observed upon addition of magnetite to chitosan nanobeads.

On the other hand, when the chitosan amount in the nanobeads is increased by a factor of three, a relatively narrower size distribution without aggregation is obtained where the average hydrodynamic diameter of nanobeads is 48 ± 2 nm, as shown in Figure 4. This result suggests that an increase in the concentration of chitosan during the synthesis lead to an increase in the hydrodynamic diameter of magnetite-chitosan nanobeads (Omar Zaki, Ibrahim, Katas, 2015; Abdayeh *et al*., 2017).

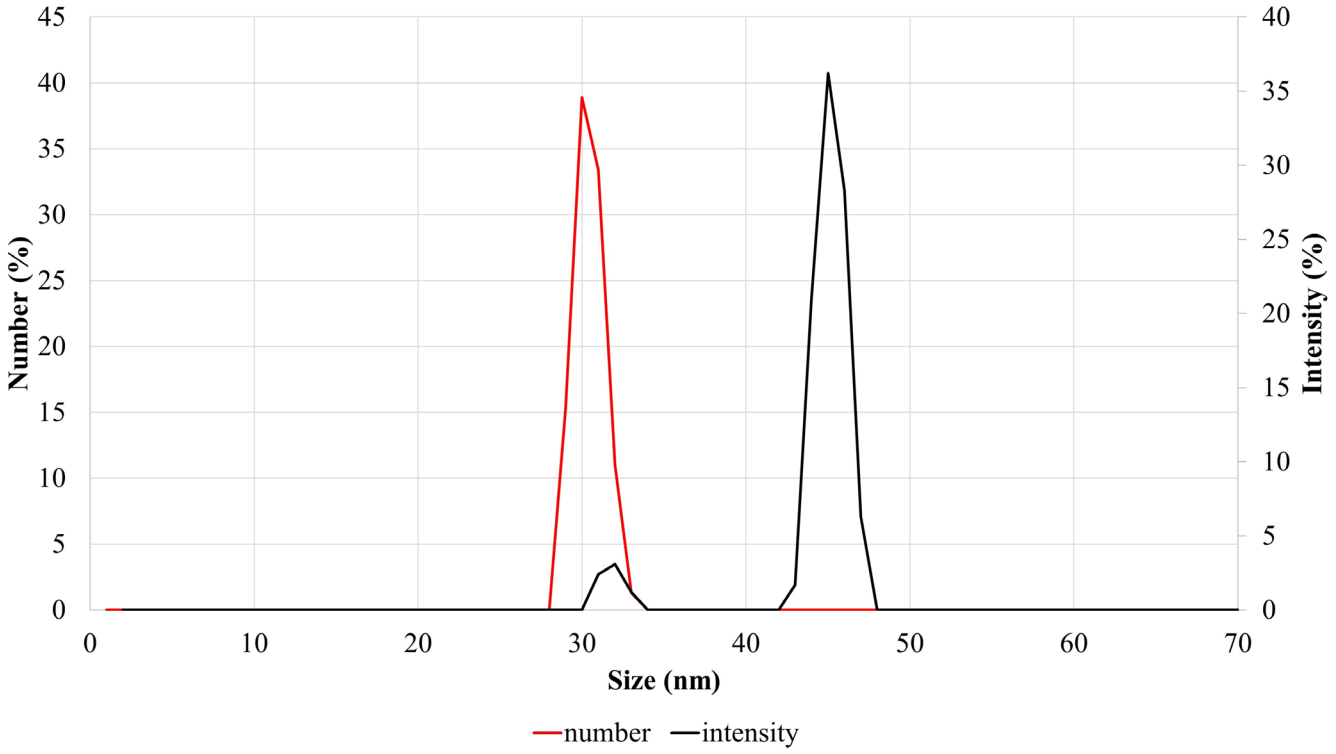

FIGURE 3 - Size distribution of magnetite-chitosan nanobeads with DLS ($[Na_2SO_4.10H_2O]_{final}$ = 1.1 wt% ; $[chitosan]_{final}$ =0.11 wt% ; salt + $[\beta$-CD coated magnetite$]_{final}$ =2.1 mg/mL). The average hydrodynamic diameter of magnetite-chitosan nanobeads are 31±2 nm and minor aggregation is suggested around 45 nm.

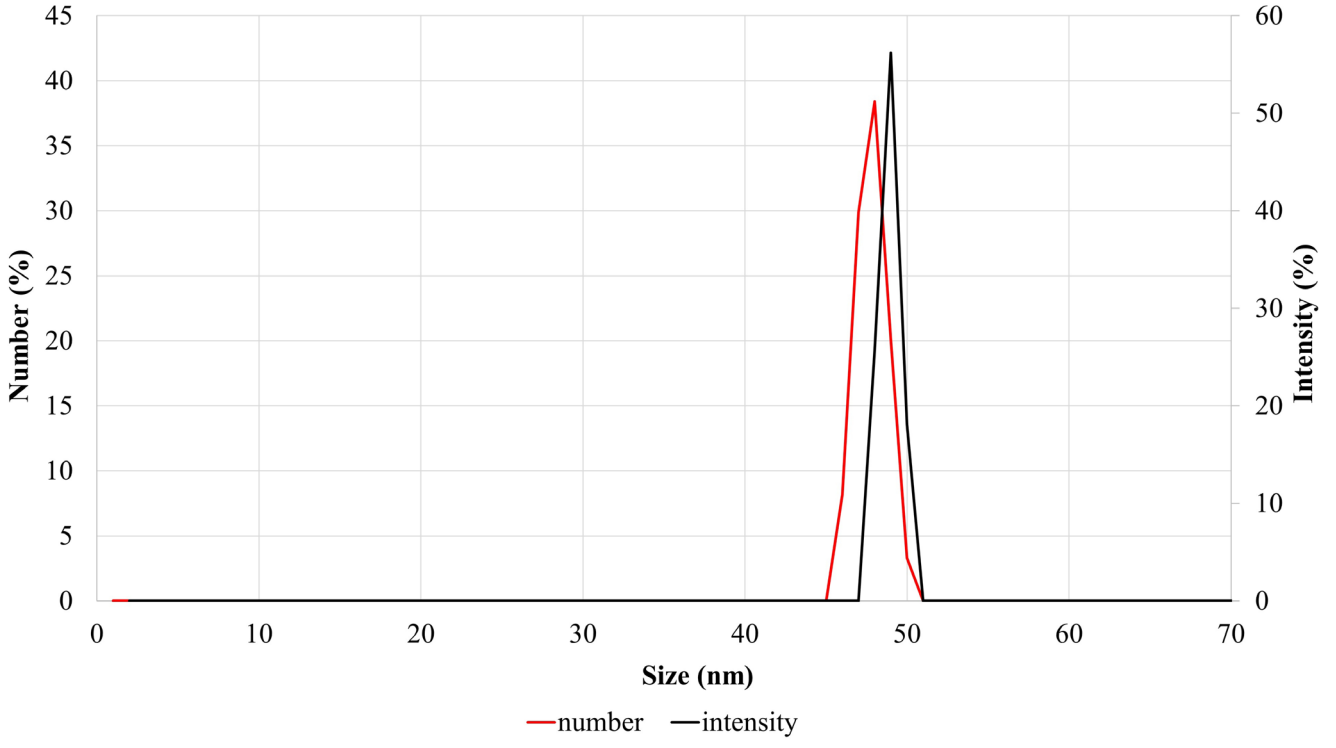

FIGURE 4 - Size distribution of magnetite-chitosan beads with DLS ($[Na_2SO_4.10H_2O]_{final}$ = 1.1 wt% ; $[chitosan]_{final}$ =0.33 wt% ; $[\beta$-CD coated magnetite$]_{final}$ =2.1 mg/mL). An increase in the chitosan amount leads to the formation of relatively larger nanobeads having narrower size distribution without further aggregation.

Magnetic properties of the magnetite-chitosan nanobeads

The suitable application of magnetic nanoparticles in magnetic drug targeting systems mostly relies on the magnetic properties of the corresponding nanoparticles. For these types of drug delivery systems, it is essential to implement particles that have optimum saturation magnetization and preferably superparamagnetic properties as the remaining magnetism in the absence of an external magnetic field may lead to aggregation due to magnetic interactions resulting in clogging within blood channels. Magnetic properties of β-CD-mag-chitosan nanobeads were measured by VSM and results clearly indicate that the obtained nanobeads containing magnetite nanoparticles have superparamagnetic properties with no coercivity and remaining magnetization. As shown in Figure 5, the saturation magnetizations of the magnetite-chitosan nanobeads are considerably lower, 30.1 emu/g and 21.4 emu/g for 0.2 wt% and 1 wt% chitosan, respectively than that of bulk magnetite (90 emu/g) (Goya, Berquó, Fonseca, 2003; Demortiere *et al*., 2011) which is due to the presence of chitosan non-magnetic layer around the magnetic core (Yuan *et al*., 2012).

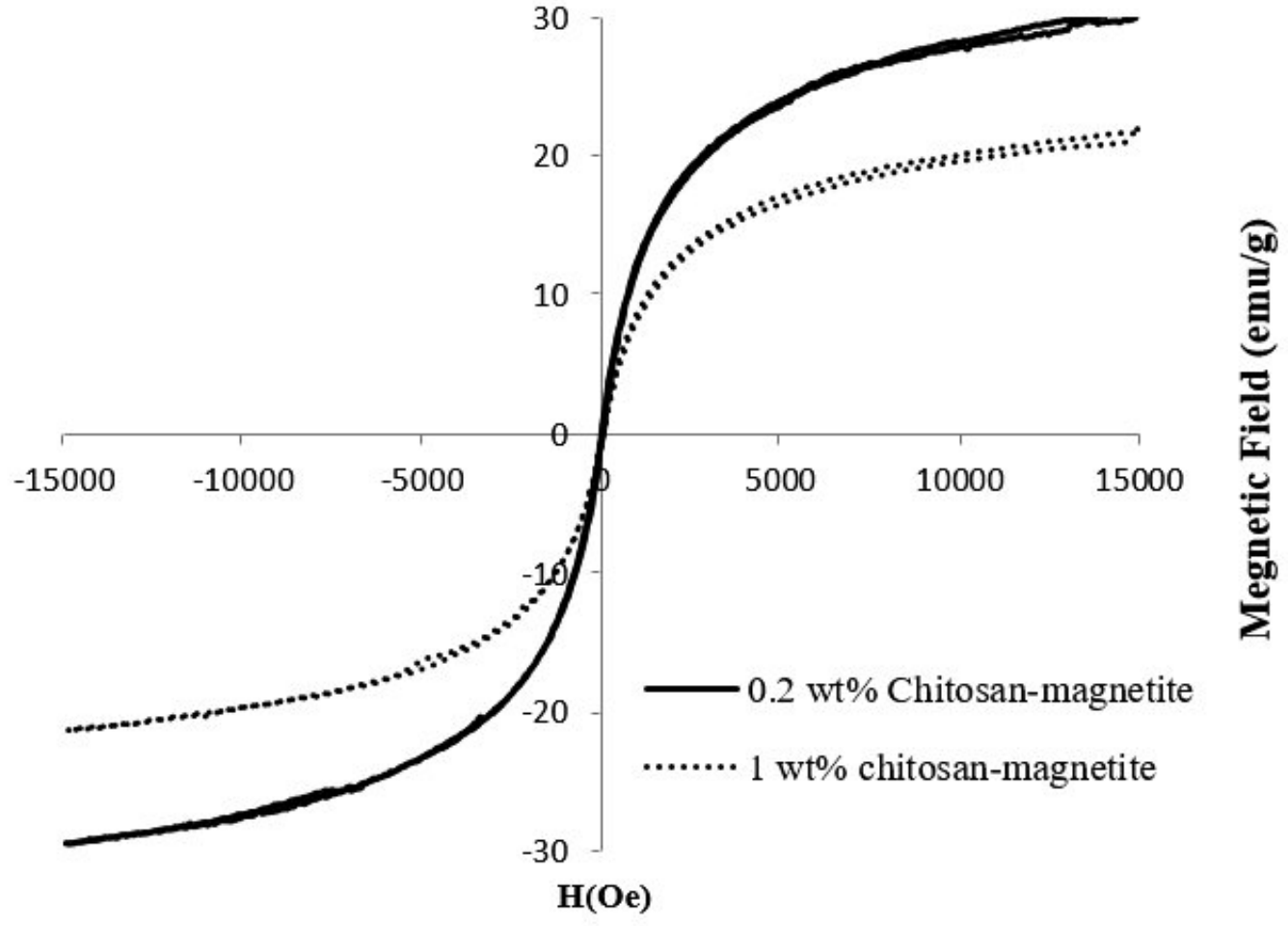

FIGURE 5 - VSM data for chitosan-magnetite nanobeads where the magnetite concentration is 3.9 mg/mL Magnetite nanoparticles that are incorporated into the nanobeads exhibit superparamagnetic properties and possess lower saturation magnetizations as expected due to non-magnetic layer around the particles.

Surface coating of magnetic nanoparticles

The obtained magnetic nanoparticles, after their synthesis in the presence of cyclodextrins, were colloidally stable, which suggests either the covalent attachment of cyclodextrins onto the surface of these particles or via electrostatic interactions at the surface. The nature of these interactions are beyond the scope of this paper, however the longevity of these colloidal particles is desired. The amounts of CDs on the surface of magnetite nanoparticles are revealed by using the thermogravimetric analysis (TGA). For these measurements, nanoparticles were washed with water and then dried in a vacuum oven at 60 ºC overnight. Bare nanoparticles show an initial weight loss of approximately 1.74 wt. % till 150 ºC which is attributed to the evaporation of adsorbed water while further weight loss of 2.63 wt. % until 600 ºC may be attributed to the impurities within the sample, as shown in Figure 6,. For the functionalized magnetite nanoparticles, the weight losses observed in the 150-600 ºC interval are due to the presence of organic layer (i.e. CD coating) on the surface of the particles

In addition, the onset temperature being unique to the compound can be used to determine the presence of coating on the particle surface. According to the weight loss profiles given in Figure 5, bare β-CD has an onset temperature of 353 ºC, which is consistent with literature, while β-CD functionalized magnetite nanoparticles have an onset temperature of 202 ºC. Additionally, weight loss profiles of H-γ-CD and H-β-CD functionalized magnetite nanoparticles have an onset temperatures of 243 ºC and 245 ºC respectively. These results clearly show that there exist temperature shifts on the onset temperatures for CD functionalized magnetite nanoparticles, indicating successful attachment of CDs onto the surface of magnetite nanoparticles. It should be

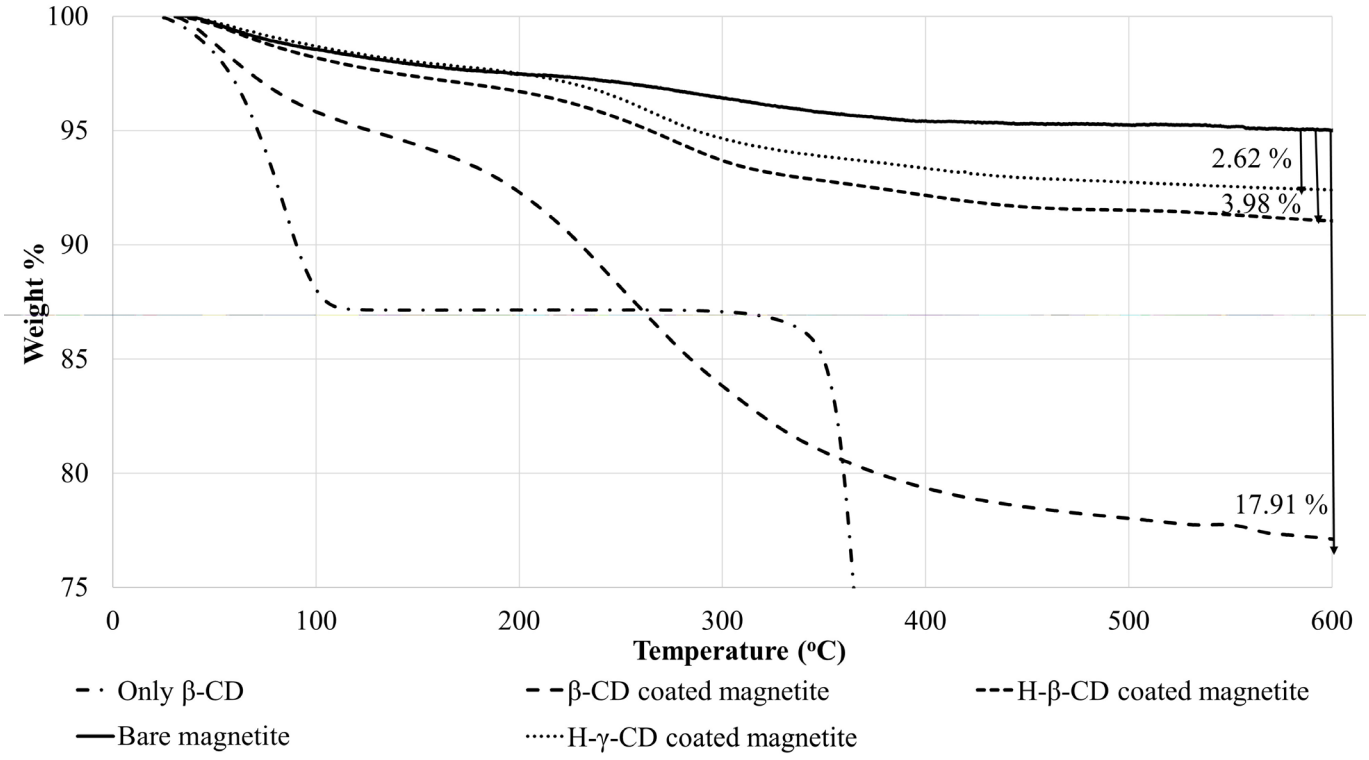

FIGURE 6 - Thermogravimetric analysis for magnetite with and without CD's. The initial weight loss observed for all samples up to ~100 – 120 ºC are attributed to the removal of adsorbed water and further losses are due to the organic layer around the particles. The highest amount of CD coating is observed for β-CD coated magnetite nanoparticles (~18%) and the wt.% difference between the two plateaus at 150 ˚C and 600 ˚C are tabulated in Table I as % coating of magnetite nanoparticles with different type of CD's.

noted that the highest amount of CD coating is achieved with β-CD (about 18 wt.% loss as compared to about 4 and 3 wt.% for H-β-CD and H-γ-CD, respectively) where the highest shift in onset temperature is also observed. As more CD molecules reside on the magnetite surface, the change in onset temperature becomes more pronounced. Finally, these results show that magnetite particles were successfully functionalized with all types of CD's but at varying coating densities.

TABLE I - Percentage coating of magnetite nanoparticles with different CD's

Type of cyclodextrins	wt. loss% (150 ºC – 600 ºC)
β-Cyclodextrin	17.91
2-hydroxy propyl-b-Cyclodextrin	3.98
2-hydroxy propyl-γ-Cyclodextrin	2.62

Encapsulation of TMZ in chitosan-magnetite nanobeads

Feasible application of magnetite-chitosan nanobeads as a drug delivery system essentially relies on the drug encapsulation efficiency of the nanobeads. Temozolomide has been encapsulated in liposomes. Although some progress in some cancer treatments has been made over the years, there is still no definitive treatment available for Glioblastoma multiforme (GBM). It has been demonstrated that the currently limited efficacy of convection-enhanced delivery (CED) could be enhanced by a liposomal formulation, thus achieving enhanced TMZ localization to the tumor site with minimal toxicity. On the other hand, a novel approach has been described for treating GBM by CED of (PEGylated) liposomes containing TMZ, the known chemotherapeutic agent (Vanza *et al*., 2018; Lin *et al*., 2018.; Nordling-David *et al*., 2017). However, to our knowledge no magnetic targeting of temozolomide is ever presented in the literature. In order to study the encapsulation extent of chemotherapeutic drug temozolomide in the magnetite-chitosan nanobeads, the concentration of CD modified magnetite nanoparticles was kept at 0.5 wt.%, and the concentration of precipitating salt and chitosan were varied. The encapsulated amount of TMZ in magnetite-chitosan nanobeads was measured by HPLC and the corresponding results are shown in Table II. At a fixed concentration of chitosan, an increase in the concentration of salt either do not alter or adversely affect the encapsulation efficiency of TMZ in magnetite-chitosan nanobeads, as shown in Table II,. Except for H-γ-CD functionalized magnetite nanoparticles, keeping the chitosan concentration 0.22 wt.% and increasing the salt concentration from 1.1 to 2.2 wt.% lead to a decrease in the encapsulated TMZ amount, whereas for higher chitosan concentrations, the encapsulated amount of drug remains essentially unaffected. For H-γ-CD functionalized magnetite nanoparticles at 1.1 wt.% final salt concentration, increasing chitosan amount results in an increase in the encapsulated TMZ amount. These results indicate that the final concentrations of chitosan and salt have a delicate balance in optimization of the amount of TMZ encapsulated in magnetite-chitosan nanobeads.

For targeting studies, TMZ loaded β-CD-magnetite-chitosan nanobeads were circulated in a closed system and for comparison collected at different test sections which have different inner diameters of 1.49 mm (Section I) and 2.19 mm (Section II), by applying 0.3 T and 0.5 T magnetic fields, respectively. Once magnetite-chitosan nanobeads are collected in the specified test sections, the amounts of chitosan, TMZ as well as magnetite nanoparticles were calculated and tabulated in Table III.

The results indicated that, when nanobead bearing nanofluid flowed within the closed system and an external magnetic field strength of 0.3 T was applied, an insignificant amount of TMZ (~0.1mg) was collected as compared to the initial amount (0.01 g) in the smaller diameter test section regardless of the concentration of chitosan and salt as shown in III. The high ratio of the collected TMZ to chitosan is an indication of the formation of a successful drug carrier and using small diameter and low magnetic field did not result in a satisfactory ratio.

To improve the amount of collected TMZ with respect to the magnetic carrier, targeting experiments were also performed by using a larger diameter test section and applying an enhanced external magnetic field strength of 0.5 T. The results shown in Table IV clearly indicate that an increase in the test section diameter as along with an increase in the external magnetic field strength increased the amount of nanobead collected, thus TMZ targeted.

TABLE II - % Encapsulated TMZ in magnetite-chitosan nanobeads comparing chitosan and salt concentrations

Final [Chitosan] (wt%)	Final [salt] (wt%)	with β-CD coated magnetite (% encapsulation)	with H-β-CD coated magnetite (% encapsulation)	with H-γ-CD coated magnetite (% encapsulation)
0.22	1.1	35.0 ± 2.8	37.0 ± 3.9	29.0 ± 2.7
0.22	2.2	16.5 ± 1.1	20.0 ± 2.4	26.0 ± 2.1
0.33	1.1	35.5 ± 7.8	39.0 ± 4.1	36.0 ± 5.2
0.33	2.2	35.0 ± 3.4	32.0 ± 4.8	19.0 ± 3.2
0.43	1.1	35.5 ± 3.5	38.0 ± 3.6	45.0 ± 5.6
0.43	2.2	37.5 ± 3.5	41.0 ± 4.2	45.0 ± 4.8

Targeting of TMZ loaded magnetite-chitosan nanobeads

TABLE III - Targeting study with Section I (applying 0.3 T magnetic field)

Final [Chitosan] (wt%)	Final [$Na_2SO_4.10H_2O$] (wt%)	Collected amount of chitosan (mg)	Captured concentration of magnetite (mg)	Collected amount of TMZ (mg)	TMZ / Chitosan
0.22	2.2	0.35± 0.03	0.28± 0.02	0.09± 0.008	0.26± 0.007
0.43	2.2	0.23± 0.02	0.09± 0.01	0.08± 0.01	0.35± 0.009
0.09	1.1	0.25± 0.02	0.49± 0.05	0.12± 0.07	0.48± 0.01
0.22	1.1	0.23± 0.03	0.18± 0.009	0.11± 0.009	0.48± 0.008
0.33	1.1	0.48± 0.04	0.25± 0.02	0.10± 0.01	0.21± 0.008

For instance, magnetite-chitosan nanobeads which have final concentrations of 0.43 wt.% and 2.2 wt.% chitosan and salt, respectively led to the collection of approximately 0.32 mg of TMZ in the test section, where the ratio of the collected TMZ to chitosan was 0.47. However, magnetite-chitosan nanobeads which contain 0.09 wt.% final chitosan and 2.2 wt.% final salt concentrations, approximately 0.27 mg was collected in the desired area and the ratio of the collected TMZ to chitosan was 1.05. Although more TMZ might be collected with higher amounts of chitosan, large ratio of collected TMZ to chitosan value is desired for efficiency. Therefore, nanobeads with low concentration of chitosan may be more suitable as nanocarriers. It is known in the literature that any matrix which is not magnetic around a magnetic material reduces the magnetizability of the carrier (Yuan *et al*., 2012). If the non-magnetic material is what carries the drug (as it is in this case), although it is tempting to increase the encapsulated amount of drug by increasing the nonmagnetic matrix, it may result in the reduction of saturation magnetization, thus the loss of ability of magnetic capture of these particles (Ghazanfari *et al*., 2016) Based on the results, an optimum concentration of 0.09 wt.% final chitosan concentration

was suggested with two different final concentrations of salt (1.1 wt.% and 2.2 wt%). It should be noted that as chitosan concentration in the nanobeads decreases, saturation magnetization of the nanobeads increases (shown with VSM results). This leads to an increase in the captured magnetite (i.e. nanobeads) amount, which is responsible for the high amount of TMZ captured with respect to the amount of novel drug carrier.

Stability studies

The colloidal stability of functionalized magnetite nanoparticles was investigated by time resolved settling experiments and compared with bare magnetite nanoparticles. Table V shows that, bare nanoparticles precipitate within 15 minutes due to lack of any surface modifications preventing agglomeration. On the other hand, all the functionalized magnetite nanoparticles showed enhanced and suitable colloidal stability where the longest stability was obtained with 2-hydroxypropyl β-CD (> 5 hours). These settling times are remarkably enhanced in acidic environment where studies with TMZ were carried out. Although some other stabilizers could be used as coating material, CDs are well-established drug carriers which are known to be not only non-toxic but also biocompatible (Bai *et al*., 2018; Garnero *et al*., 2018; Kim *et al*., 2018).

TABLE V - Settle time for different CDs coated magnetic nanoparticles

Sample	Time to Precipitation
Bare magnetite	15 minutes
Magnetite with β-CD	55 minutes
Magnetite with	> 5 hours
Magnetite with	40 minutes

Cytotoxicity studies

In vitro cytotoxicity studies were performed for both bare and β-CD coated magnetite nanoparticles (β-CD-mag) as well as b-CD-mag-chitosan nanobeads. As functionalized magnetite nanoparticles are intended to be used for biomedical applications, it is important that they do not possess toxicity for cells. Figure 6 shows the viability of cells after three days and it is clearly observed that bare magnetite nanoparticles do not exhibit toxicity at least until 330 μg/mL. On the other hand, cell viability was further enhanced upon functionalization of these particles with various types of CDs (almost up to 800 μg/mL). In the literature, superparamagnetic magnetite nanoparticles

TABLE IV - Targeting study with Section II (applying 0.5 T magnetic field)

Final [Chitosan] (wt%)	Final [$Na_2SO_4.10H_20$] (wt%)	Collected amount of chitosan (mg)	Captured amount of magnetite (mg)	Collected amount of TMZ (mg)	
0.09	1.1	0.32 ± 0.01	0.63 ± 0.01	0.27 ± 0.03	0.82 ± 0.09
0.09	2.2	0.26 ± 0.02	0.51 ± 0.04	0.27 ± 0.01	1.05 ± 0.05
0.22	1.1	0.72 ± 0.03	0.56 ± 0.02	0.33 ± 0.02	0.44 ± 0.01
0.22	2.2	0.33 ± 0.02	0.26 ± 0.02	0.25 ± 0.02	0.75 ± 0.08
0.33	1.1	0.84 ± 0.06	0.44 ± 0.03	0.31 ± 0.03	0.37 ± 0.07
0.33	2.2	0.73 ± 0.09	0.38 ± 0.05	0.29 ± 0.01	0.53 ± 0.20
0.43	1.1	0.52 ± 0.14	0.21 ± 0.05	0.27 ± 0.03	0.53 ± 0.15
0.43	2.2	0.68 ± 0.17	0.27 ± 0.07	0.32 ± 0.05	0.47 ± 0.05

was shown to have a dose dependent toxicity (Darroudi *et al*., 2014) while ferromagnetic magnetite nanoparticles were shown to be non-toxic up to 1000 µg/mL, where biocompatibility was enhanced upon coating with PAA polymer (Altan *et al*., 2016). Chitosan has been used in biomedical applications for decades. Chitosan is an effective material for biomedical applications because of its biocompatibility, biodegradability and non-toxicity, apart from their antimicrobial activity and low immunogenicity. Chitosan-based biomaterials have become a popular target in the development of tissue engineering and significant progress has recently been made. It provides certain mechanical and structural properties for proper functioning for the repaired tissues (Khan *et al*., 2018; Fiqrianti *et al*., 2018; Sun, Lee, Zhang, 2018).

Encapsulation of β--CD coated magnetite nanoparticles in chitosan nanobeads further increased the biocompatibility of the particles (non-toxic up to 2000 µg/mL), leading to a promising magnetic carrier for biomedical applications, as seen in Figure 7,.

CONCLUSION

The chemotherapeutic drug, TMZ which is often employed against brain cancers is encapsulated in a magnetic carrier, where chitosan is the drug embedded polymer and magnetite nanoparticles are responsible for the magnetic targeting.

Magnetite nanoparticles, synthesized by the coprecipitation method are surface modified with CDs which are hydrophilic molecules with hydrophobic cavities, to accommodate TMZ. These magnetic nanoparticles are then embedded in chitosan nanobeads prepared by salt addition. Magnetic properties of the developed vehicle are shown to be sufficient to accumulate the nanocarrier (i.e. magnetic nanobeads) in

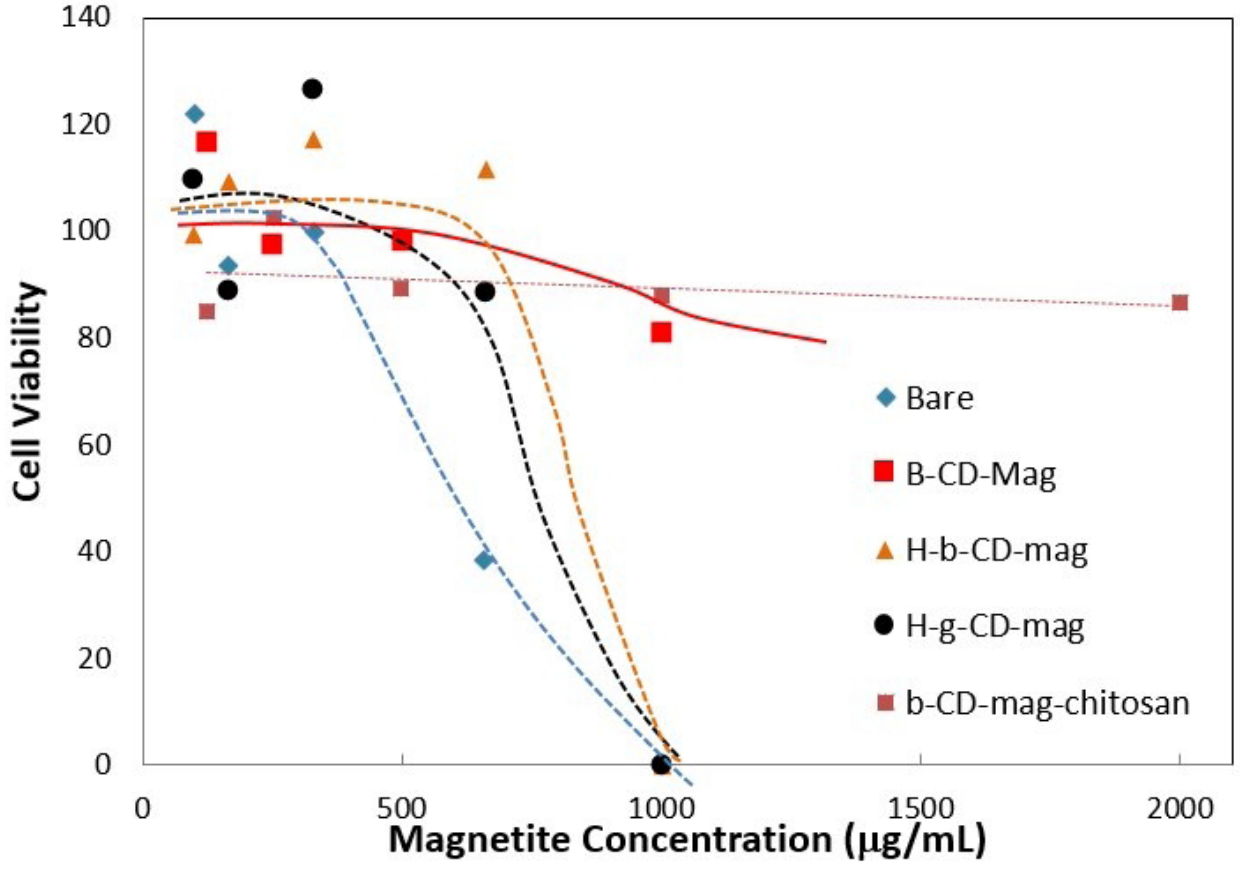

FIGURE 7 - Cell Viability versus magnetite concentration for CD-coated magnetite nanoparticles and chitosan embedded magnetite nanobeads. The connecting lines are placed as a guide to the eye. Magnetite nanoparticles do not possess toxicity of up to 330 µg/mL, while viability further increased after functionalization of particles by different types of CDs. Encapsulation of β-CD functionalized magnetite nanoparticles in chitosan nanobeads further increased the biocompatibility of the particles.

a target area by the application of the 0.5 T magnetic field, which makes these particles suitable for targeted drug delivery applications.

Experimental conditions are optimized to maximize the amount of targeted TMZ, minimizing the amount of chitosan used in the nanobead. An optimum concentration of 0.09 wt.% final chitosan concentration can be suggested at a final salt concentration of 2.2 wt%. As the chitosan amount increases with respect to magnetite, the magnetic properties of the carrier decrease which diminishes the ability to target these nanobeads in the desired area. Therefore, a delicate balance between the amount of TMZ, magnetite and chitosan exists. To our knowledge this is the first study which shows that TMZ can be targeted using a suitable nanocarrier.

REFERENCES

Abyadeh M, Zarchi AAK, Faramarzi MA, Amani A. Evaluation of factors affecting size and size distribution of chitosan-electrosprayed nanoparticles. Avicenna J Med Biotechnol. 2017;9(3) 126-132.

Agarwala SS, Kirkwood JM. Temozolomide, a novel alkylating agent with activity in the central nervous system, may improve the treatment of advanced metastatic melanoma. Oncologist. 2000;5(2):144-151.

Altan CL, Gurten B, Sadza R, Yenigul E, Sommerdijk NAJM, Bucak S. Poly(acrylic acid)-directed synthesis of colloidally stable single domain magnetite nanoparticles via partial oxidation. J Magn Magn Mater. 2016;416:366-372.

Andrade-Eiroa A, Canle M, Leroy-Cancellieri V, Cerdà V. Solid-phase extraction of organic compounds: A critical review (Part I). Trends Analyt Chem. 2016;80:641-654.

Andrasi M, Bustos R, Gaspar A, Gomez FA, Klekner A. Analysis and stability study of temozolomide using capillary electrophoresis. J Chromatogr B Analyt Technol Biomed Life Sci. 2010;878(21):1801-1808.

Bagot JL. Okoubaka aubrevillei. A new homeopathic medicine for the side effects of chemotherapy. La Revue d'Homéopathie. 2015;6(2):e1-e6.

Bai S, Hou M, Shi X, Chen J, Ma X, Gao YE, Wang Y, Xue P, Kang Y, Xu Z. Reduction-active polymeric prodrug micelles based on α-cyclodextrin polyrotaxanes for triggered drug release and enhanced cancer therapy. Carbohydr Polym. 2018;193:153-162.

Baker SD, Wirth M, Statkevich P, Reidenberg P, Alton K, Sartorius SE, et al. Absorption, metabolism, and excretion of 14C-temozolomide following oral administration to patients with advanced cancer. Clin Cancer Res. 1999;5(2):309-317.

Bano S, Afzal M, Waraich MM, Alamgir K, Nazir S. Paclitaxel loaded magnetic nanocomposites with folate modified chitosan/carboxymethyl surface; a vehicle for imaging and targeted drug delivery. Int J Pharm. 2016;513(1-2):554-563.

Brada M, Judson I, Beale P, Moore S, Reidenberg P, Statkevich P, et al. Phase I dose-escalation and pharmacokinetic study of temozolomide (SCH 52365) for refractory or relapsing malignancies. Br J Cancer. 1999;81(6):1022-1030.

Chidambaram M, Manavalan R, Kathiresan K. Nanotherapeutics to overcome conventional cancer chemotherapy limitations. J Pharm Pharm Sci. 2011;14(1):67-77.

Coolbrandt A, Van den Heede K, Vanhove E, De Bom A, Milisen K, Wildiers H. Immediate versus delayed self-reporting of symptoms and side effects during chemotherapy: Does timing matter? Eur J Oncol Nurs. 2011;15(2):130-136.

Darroudi M, Hakimi M, Goodarzi E, Oskuee RK. Superparamagnetic iron oxide nanoparticles (SPIONs): Green preparation, characterization and their cytotoxicity effects. Ceram Int. 2014;40(9 Pt B):14641-14645.

Del Valle EMM. Cyclodextrins and their uses: a review. Process Biochem. 2004;39(9):1033-1046.

Demortière A, Panissod P, Pichon BP, Pourroy G, Guillon D, Donnio B, et al. Size-dependent properties of magnetic iron oxide nanocrystals. Nanoscale. 2011;3(1):225-232.

Eastburn SD, Tao BY. Applications of modified cyclodextrins. Biotechnol Adv. 1994;12(2):325-339.

Fiqrianti IA, Widiyanti P, Manaf MA, Savira CY, Cahyani NR, Bella FR. Poly-L-lactic Acid (PLLA)-Chitosan-collagen electrospun tube for vascular graft application. J Funct Biomater. 2018;30;9(2):E32.

Garnero C, Chattah AK, Aloisio C, Fabietti L, Longhi M. Improving the stability and the pharmaceutical properties of norfloxacin form C through binary complexes with β-cyclodextrin. AAPS PharmSciTech. 2018;19(5):2255-63.

Ghazanfari MR, Kashefi M, Shams SF, Jaafari MR. Perspective of Fe_3O_4 nanoparticles role in biomedical applications. Biochem Res Int. 2016;2016:7840161.

Goya GF, Berquó TS, Fonseca FC. Static and dynamic magnetic properties of spherical magnetite nanoparticles. J Appl Phys. 2003;94(5):3520-3528.

Hakkarainen B, Fujita K, Immel S, Kenne L, Sandström C. 1H NMR studies on the hydrogen-bonding network in mono-altro-beta-cyclodextrin and its complex with adamantane-1-carboxylic acid. Carbohydr Res. 2005;340(8):1539-1545.

Hamzelou J. Drug wipes out chemotherapy side effects. New Sci. 2017;233(3112):16.

Huang G, Zhang N, Bi X, Dou M. Solid lipid nanoparticles of temozolomide: potential reduction of cardial and nephric toxicity. Int J Pharm. 2008;355(1):314-320.

Jain D, Gursalkar T, Bajaj A. Nanosponges of an anticancer agent for potential treatment of brain tumors. Am J Neuroprot Neuroregen. 2013;5(1):32-43.

Janko C, Zaloga J, Pöttler M, Dürr S, Eberbeck D, Tietze R, et al. Strategies to optimize the biocompatibility of iron oxide nanoparticles – "SPIONs safe by design. J Magn Magn Mater. 2017;431:281-284.

Khan A, Aqil M, Imam SS, Ahad A, Sultana Y, Ali A, Khan K. Temozolomide loaded nano lipid based chitosan hydrogel for nose to brain delivery: Characterization, nasal absorption, histopathology and cell line study. Int J Biol Macromol. 2018;116:1260-7.

Kim H, Likhari P, Parker D, Statkevich P, Marco A, Lin CC, et al. High-performance liquid chromatographic analysis and stability of anti-tumor agent temozolomide in human plasma. J Pharm Biomed Anal. 2001;24(3):461-468.

Kim YH, Kim ST, Jee JP, Kim DY, Kang D, Kim K, Park SY, Sim T, Cho KH, Jang DJ. Removing control of cyclodextrin-drug complexes using high affinity molecule. J Nanosci Nanotechnol. 2018;18(2):898-901.

Kleine A, Altan CL, Yarar UE, Sommerdijk NAJM, Bucak S, Holder SJ. The polymerisation of oligo (ethylene glycol methyl ether) methacrylate from a multifunctional poly (ethylene imine) derived amide: a stabiliser for the synthesis and dispersion of magnetite nanoparticles. Polym Chem. 2014;5(2):524-534.

Kumar R, Inbaraj BS, Chen BH. Surface modification of superparamagnetic iron nanoparticles with calcium salt of poly (γ-glutamic acid) as coating material. Mater Res Bull. 2010;45(11):1603-1607.

Lin CY, Li RJ, Huang CY, Wei KC, Chen PY. Controlled release of liposome-encapsulated temozolomide for brain tumour treatment by convection-enhanced delivery. J Drug Target. 2018;26(4):325-332.

Marchesi F, Turriziani M, Tortorelli G, Avvisati G, Torino F, De Vecchis L. Triazene compounds: mechanism of action and related DNA repair systems. Pharmacol Res. 2007;56(4):275-287.

Nam JP, Park SC, Kim TH, Jang JY, Choi C, Jang MK, et al. Encapsulation of paclitaxel into lauric acid-O-carboxymethyl chitosan-transferrin micelles for hydrophobic drug delivery and site-specific targeted delivery. Int J Pharm. 2013;457(1):124-135.

Nordling-David MM, Yaffe R, Guez D, Meirow H, Last D, Grad E, Salomon S, Sharabi S, Levi-Kalisman Y, Golomb G, Mardor Y. Liposomal temozolomide drug delivery using convection enhanced delivery. J Control Release. 2017;261:138-146.

Omar Zaki SS, Ibrahim MN, Katas H. Particle size affects concentration-dependent cytotoxicity of chitosan nanoparticles towards mouse hematopoietic stem cells. J Nanotechnol. 2015;2015:919658.

Parida UK, Bindhani BK. Cross-linked Chitosan-Sodium Sulfate Matrix Systems Using Gel Casting Method for Sustained Drug Release of Doxorubicin Hydrochloride. Int J Drug Deliv. 2015;7(2):101-112.

Patil RM, Shete PB, Thorat ND, Otari SV, Barick KC, Prasad A, et al. Superparamagnetic iron oxide/chitosan core/shells for hyperthermia application: Improved colloidal stability and biocompatibility. J Magn Magn Mater. 2014;355:22-30.

Petcharoen K, Sirivat A. Synthesis and characterization of magnetite nanoparticles via the chemical co-precipitation method. Mater Sci Eng B. 2012;177(5):421-427.

Qi J, Yao P, He F, Yu C, Huang C. Nanoparticles with dextran/chitosan shell and BSA/chitosan core- Doxorubicin loading and delivery. Int J Pharm. 2010;393(1-2):177-185.

Riva R, Ragelle H, Rieux A, Duhem N, Jerome C, Preat V. Chitosan and Chitosan Derivatives in Drug Delivery and Tissue Engineering. In: Jayakumar R, Prabaharan M, Muzzarelli RAA, editors. Chitosan for Biomaterials II. Verlag Berlin Heidelberg: Springer; 2011. p. 1-18.

Saita K, Nagaoka S, Horikawa M, Shirosaki T, Matsuda S, Ihara H. Chitosan Sub-micron Particles Prepared Using Sulfate Ion Salt as Bacteriostatic Materials in Neutral pH Condition. J Biomater Nanobiotechnol. 2011;2(4):347-352.

Schwertmann U, Cornell RM. The Iron Oxides, Structure, Properties, Reactions, Occurrences and Uses. Weinheim: Wiley-VCH Verlag GmbH & Co. KGaA; 2006.

Shaterabadi Z, Nabiyouni G, Soleymani M. High impact of in situ dextran coating on biocompatibility, stability and

magnetic properties of iron oxide nanoparticles. Mater Sci Eng C. 2017;75:947-956.

Song W, Tang Z, Li M, Lv S, Sun H, Deng M, et al. Polypeptide-based combination of paclitaxel and cisplatin for enhanced chemotherapy efficacy and reduced side-effects. Acta Biomater. 2014;10(3):1392-1402.

Stupp R, Mason WP, van den Bent MJ, Weller M, Fisher B, Taphoorn MJ, et al. Radiotherapy plus concomitant and adjuvant temozolomide for glioblastoma. N Engl J Med. 2005;352(10):987-996.

Sun C, Lee JS, Zhang M. Magnetic nanoparticles in MR imaging and drug delivery. Adv Drug Deliv Rev. 2008;60(11):1252-1265.

Swaminathan S, Cavalli R, Trotta F. Cyclodextrin-based nanosponges: a versatile platform for cancer nanotherapeutics development. Wiley Interdiscip Rev Nanomed Nanobiotechnol. 2016;8(4):579-601.

Tiwari G, Tiwari R, Rai AK. Cyclodextrins in delivery systems: Applications. J Pharm Bioallied Sci. 2010;2(2):72-79.

Vanza J, Jani P, Pandya N, Tandel H Formulation and statistical optimization of intravenous temozolomide-loaded PEGylated liposomes to treat glioblastoma multiforme by three-level factorial design. Drug Dev Ind Pharm. 2018;44(6):923-933.

Yoe JH, Jones AL. Colorimetric determination of iron with disodium-1, 2-dihydroxybenzene-3, 5-disulfonate. Ind Eng Chem Anal Ed. 1944;16(2):111-115.

Yuan Y, Rende D, Altan CL, Bucak S, Ozisik R, Borca-Tasciuc D. Effect of Surface Modification on Magnetization of Iron Oxide Nanoparticle Colloids. Langmuir. 2012;28(36): 13051-13059.

Zuckerman JE, Hsueh T, Koya RC, Davis ME, Ribas A. siRNA knockdown of ribonucleotide reductase inhibits melanoma cell line proliferation alone or synergistically with temozolomide. J Invest Dermatol. 2011;131(2):453-460.

Received for publication on 20th July 2018
Accepted for publication on 23rd September 2018